Computational Aeroacoustics Simulation of an Air Micro-Injector with Dimples Shape on the Surface of Divergent Nozzle

Jun Liu[1*], Toshiharu Kagawa[2]

[1] *Keihin-Corp., Hoshakuji, 2021-8, Takanezawa-machi, Shioya-gun, Tochigi, 329-1233, Japan*
[2] *Tokyo Institute of Technology, 4259 Nagatsuta-cho, Midori-ku, Yokohama 226-8503, Japan*
[*] liujun3@hotmail.com (corresponding author e-mail)

Abstract. As for jet noise reduction of an air micro-injector with divergent nozzle, dimples shape in the inner surface of divergent nozzle is proposed, in the paper, the jet noise reduction effect of dimples shape is numerically confirmed at delivery pressure 1.33 atm. and 2.0 atm. (fully expanded jet Mach number 0.65 and 1.05), using Ffows Williams and Hawkings (FW-H) method base on time-accurate solutions of Large-Eddy Simulation (LES). In addition, the influence of dimples nozzle on the jet flow field is numerically investigated.

1. Introduction

Recently, jet noise is an interesting and important topic in fluid mechanics, and has received much attention from scientists and engineers. On the one hand, for scientists, the ultimate goal is elucidation of the fluid dynamic mechanisms for noise generation and construction of jet noise prediction methodology. On the other hand, engineers are significant concern in jet noise reduction. However, an understanding of noise generation mechanisms may be helpful in guiding noise reduction studies.

The early investigations on jet noise were started by Lighthill [1], where the total acoustic power of the jet is obtained with the eight power of jet velocity, and the eight power law matches surprisingly well with many jet experiments, e.g. Viswanathan [2], and thereafter, the most general form of the Lighthill acoustic analogy were developed by several studies, Ffows Williams [3] accounted the effect that the turbulent eddies that give rise to the Reynolds stresses are convected by jet velocity and their motion alters the radiated sound, the refraction effect of the mean jet velocity on sound is investigated by Mani [4] and Colonius [5], and a more accurate acoustic formulation of linear propagation effects is discussed by Goldstein [6], the nonlinear problems of sound generation is challenged by Colonius [7].

For high-speed jets, the different of jet-noise properties at small and large observation angles to the flow are studied in numerous experimental and numerical investigations, e.g. Tam [8,9,10], Morris [11,12] and Viswanathan [13], they found that the fitting functions for high observer angles are referred to as the fin-scale spectrum (FSS) and the large-scale spectrum (LSS) for the small observer angles, and the semi-empirical two-source FSS-LSS model is suggested.

Nowadays, because of the rapid development of computers and in particular the growing computational power, Computational fluid dynamics (CFD) / Computational aeroacoustics (CAA) has been very successful in solving fluid and acoustic problem for industrial applications. Direct numerical simulation (DNS) has been used to predict radiated noise from turbulent flows at low Reynolds numbers by Freund [14,15], and large eddy simulation (LES) is attractive for higher Reynolds number applications, e.g. chevron nozzle by Ali Uzun [16], beveled nozzle by Viswanathan [17], dual nozzle by Michael [18], cold and hot nozzle by Bodony [19], rectangular jet by Nichols [20], convergent–divergent nozzle by Liu [21], etc.

In the paper, attention is focused on jet noise reduction of an air micro-injector that in use for blowing away the metal powder on the machined surface (e.g. hole drilling in Aluminum) in small town factory, in many cases, jet noise of air micro-injector is a large component of ambient noise levels that in pair worker comfort and productivity, and so for reduction of jet noise level, a dimples shape in the inner surface of divergent nozzle is considered, a computational aeroacoustics simulations of this air injector is presented to confirm the jet noise reduction effect of dimples nozzle, using FW-H acoustic analogy method base on transient jet flow solutions of LES, and furthermore, the influence of dimples nozzle on the jet flow field is numerically investigated.

2. Simulation Method

2.1. Physical Model

An air micro-injector used in the study was a long injection tube with divergence nozzle and a short delivery large diameter tube, for jet noise reduction, dimples shape is engraved on the inner surface of divergence nozzle, Fig.1 shows the parameters of injector configuration in detail, injection tube length is 21mm (including divergence nozzle length 5mm), and delivery tube length is 4mm, diverging angle of nozzle is 8 deg., and the dimples shape is consist of 15 dents that its radius is 0.4 mm, the inner diameter of injection tube D_j and delivery tube D_t, are 2.5mm and 5.0mm, respectively.

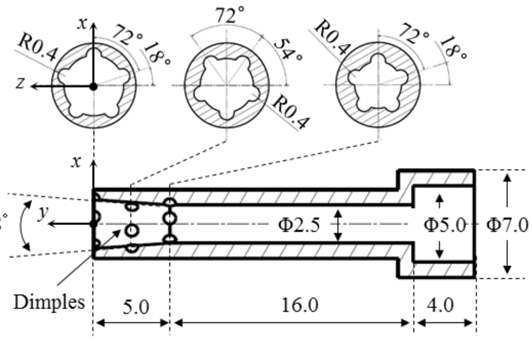

Fig.1 An air micro-injector with dimples shape on the inner surface of divergence nozzle

Here, two cases of delivery pressure are considered such as 1.33 atm. and 2.0 atm., and the fully expanded jet Mach number corresponding to delivery pressure are obtained as 0.65 and 1.05, using follows formula

$$M_j = \sqrt{\frac{2}{\kappa - 1}\left\{\left(\frac{p_1}{p_a}\right)^{\frac{\kappa-1}{\kappa}} - 1\right\}} \quad , \tag{1}$$

where, κ which is specific heat ratio, equals 1.4 in case of air, p_1 is delivery pressure and p_a is atmospheric pressure.

2.2. Numerical Method

Due to dimples shape on the inner surface of divergent nozzle, it is obviously non-axisymmetric jet flow, three-dimensional computational domain is dealt with a prolate spheroid, air injector is fixed a pole of spheroid, the major axis which is arranged along air jet direction is $110D_j$ (275 mm), and the minor axis is $80D_j$ (200 mm).

Jet noise is generated from jet flow, which is governed by well-known mass conservation and Navier-Stokes momentum equations as follows

$$\frac{\partial \rho}{\partial t}+\frac{\partial \rho u_i}{\partial x_i}=0 \quad , \tag{2}$$

$$\frac{\partial \rho u_i}{\partial t}+\frac{\partial \rho u_i u_j}{\partial x_i}=-\frac{\partial p}{\partial x_i}+\frac{\partial \sigma_{ij}}{\partial x_i} \quad , \tag{3}$$

where, ρ is density, u_i and u_j are the velocity components, p is the statistic pressure, and σ_{ij} is the viscous stress tensor as

$$\sigma_{ij}=\mu\left[\frac{\partial u_i}{\partial x_j}+\frac{\partial u_j}{\partial x_i}-\frac{2}{3}\left(\frac{\partial u_k}{\partial x_k}\right)\delta_{ij}\right] \quad , \tag{4}$$

where, δ_{ij} is Kronecker delta.

For the turbulence simulation, the air was set up as a compressible ideal-gas with temperature 20 degrees Celsius so that boundary conditions for air outflow from computational domain were defined as atmospheric pressure P_a, and the injection pressure on the jet inlet is given as delivery pressure P_1. The first step, a steady-state solution of jet flow was obtained by realizable k-ε turbulent model, and the second step, LES of unsteady air jet flow was carried out on time step (1×10^{-5} sec.) to total time step 2.0×10^{-1} sec. with which subgrid-scal model is chosen dynamics Smagorinsky-Lilly model, and the Werner-Wengle wall function [22] is used on the wall surface of the air injector.

For the acoustic computation, the mid- and far-field formulation of the permeable FW-H surface integral method is used base on transient jet flow solutions of LES, time-accurate solutions of the jet flow field variables, such as pressure, velocity components and density on the selected interior (permeable) surface, are required to evaluate the permeable surface integrals (monopole & dipoles sound source) and partially volume integrals (quadrupoles sound source within the region enclosed by the permeable surface), and the sound pressure in the acoustic observation point is given as

$$\begin{aligned}p'(\mathbf{x},t)=&\frac{1}{4\pi a_0^4}\int_V \frac{(x_i-y_i)(x_j-y_j)}{R^3}\frac{\partial^2 T_{ij}(\mathbf{y},t')}{\partial t'^2}dV(\mathbf{y})+\frac{1}{4\pi a_0}\int_S \frac{(x_i-y_i)l_i}{R^2}\frac{\partial p(\mathbf{y},t')}{\partial t'}dS(\mathbf{y})\\&+\frac{1}{4\pi}\int_S \frac{(x_i-y_i)l_i}{R^3}p(\mathbf{y},t')dS(\mathbf{y})\end{aligned} \quad , \tag{5}$$

where, T_{ij} is the Lighthill stress tensor as $T_{ij}=\rho u_i u_j-\sigma_{ij}+p_0\delta_{ij}$, a_0 is speed of sound, $\mathbf{x}(x_i, x_j)$ is the acoustic observation point where acoustic quantities are measured, $\mathbf{y}(y_i, y_j)$ is the point in the flow field where sound is generated, $R=|\mathbf{x}-\mathbf{y}|$ is therefore the distance between the acoustic observation point and the point in the flow field where sound is generated, l_j is the unit direction vector of the solid boundary, pointing toward the fluid, t is the current observation time measured at $\mathbf{x}$, respectively.

Since the permeable FW-H surface integral method is only enable to account for the contributions from the quadrupoles source (volume integral) enclosed by permeable surface, and does not include external quadrupoles source in the region outside the permeable surface, in the case of jet noise, it is necessary to select the permeable surface through the jet far downstream of the jet exit, which encloses all quadrupoles source from fine grain turbulence and large scale turbulence of turbulence jet flow (e.g. see the discussion in Michael et al. [18]). Therefore, in the paper, two integral surfaces with conical divergence of S_1=20 deg. and S_2=50 deg. which around jet flow are considered as shown in Fig.2a, and the influence of different integral surface on acoustic result is investigated by comparing with each other.

Here, 15 observation points were assumed set-up on an arc at a distance of 150 mm from the nozzle exit, and they were placed 10 deg. apart from 10 deg to 170 deg. as shown in Fig.2b.

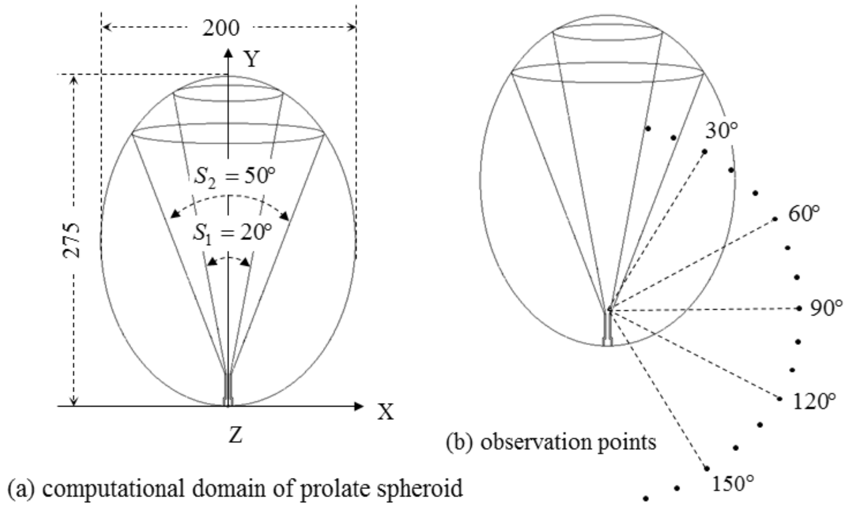

Fig.2 Computational domain (a) and acoustic observation points (b)

In case of using the permeable surface, the mesh resolution needs to be fine enough to resolve the transient flow structures inside the volume enclosed by permeable surface, the computing mesh grid of turbulent simulation was generated, and it also needs a fine distribution mesh at interior of dimples nozzle, due to which the numerical result is sufficiently accurate for estimate the influence of dimples geometric configuration on the turbulent jet flow, see in Fig.3, there are 2.56 million meshes for injector with dimples nozzle and 1.98 million meshes for base injector without dimples, respectively.

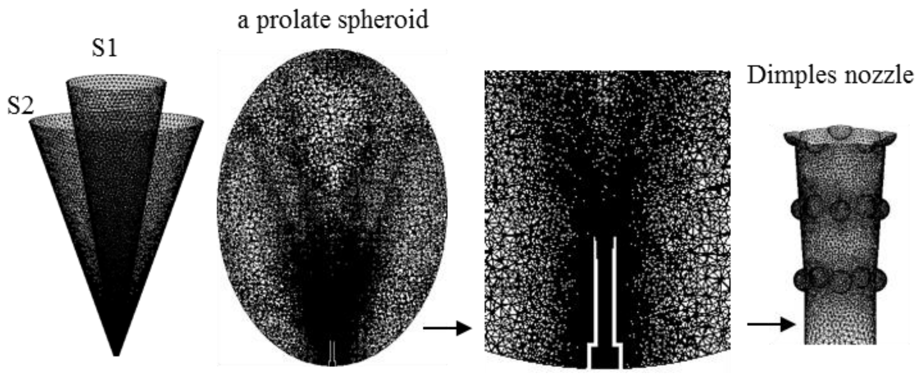

Fig.3 A fine distribution mesh at interior of dimples nozzle and permeable surface

3. Results and Discussion

In the section, first, the influence of dimples nozzle on the jet flow field is numerically investigated. Second, followed by discussion of acoustic result in the different FW-H surface, the jet-noise reduction efficiency of dimples nozzle is numerically confirmed with variation of observer points.

3.1. Numerical Results of Flow Filed

LES of unsteady air jet flow simulation was carried out by the commercial software FLUENT version 14.5, numerical solution convergence was determined by the mass flow rate and velocity components, the numerical solution was considered converged when these values changed less than 0.01% at every time step.

Figures 4a-4b display the contours of static pressure in the jet-center plane (xy-plane at z=0 and zy-plane at x=0), and the oscillation of static pressure with along the centerline of air micro-injector is plotted as shown in Fig.5, it shows that oscillation of static pressure is greatly reduced due to dimples effect in case of M_j=0.65, but in the case of M_j=1.05, oscillation of static pressure is increased at jet exit in reverse.

Additionally, the variations of axial velocity and logarithmic vorticity with along centerlines axial of jet flow are plotted as shown in Fig.6-7, it is clear that the vorticity magnitude is great reduced due to drag reduction effect of dimples configuration in the inner region of nozzle (y/Dj = -5 ~ 0), and in the region of nozzle exit, the axial velocity and vorticity of base nozzle are decreased more quickly than that of dimples nozzle in the case of M_j=0.65. Figures 8a-8b display the contours of vorticity near nozzle exit in the xy-plane at z=0 and zy-plane at x=0, where FW-H surface S_1 and S_2 are expressed as the white dashed lines, it can be found that dimples shape reduces turbulence in case of subsonic jet-flow (M_j=0.65), but the turbulence near nozzle exit is enhanced by dimples nozzle in case of supersonic jet-flow (M_j=1.05).

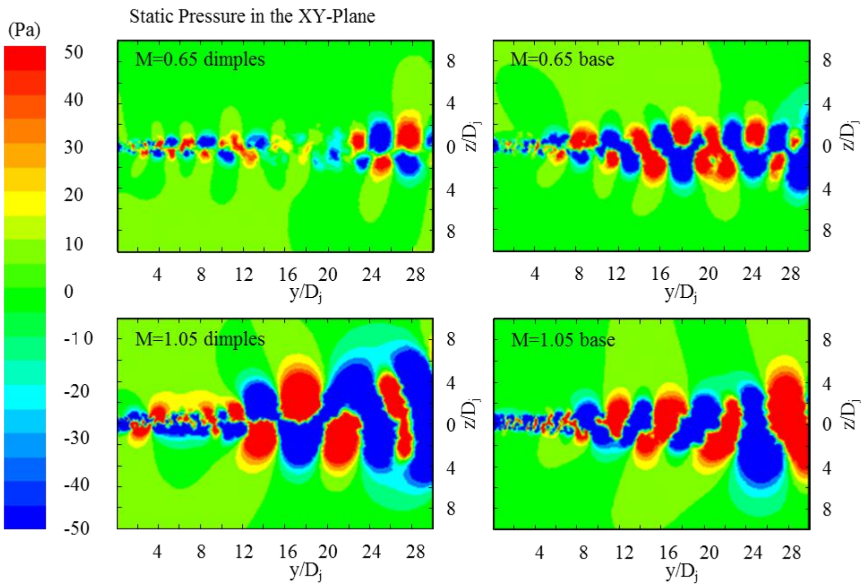

Fig.4a. Distribution of static pressure in the XY-Plane

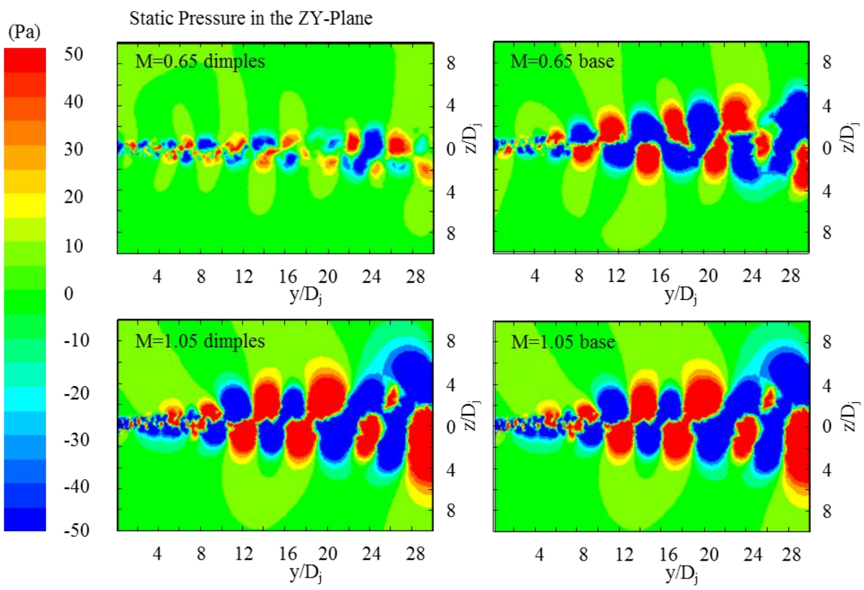

Fig.4b. Distribution of static pressure in the ZY-Plane

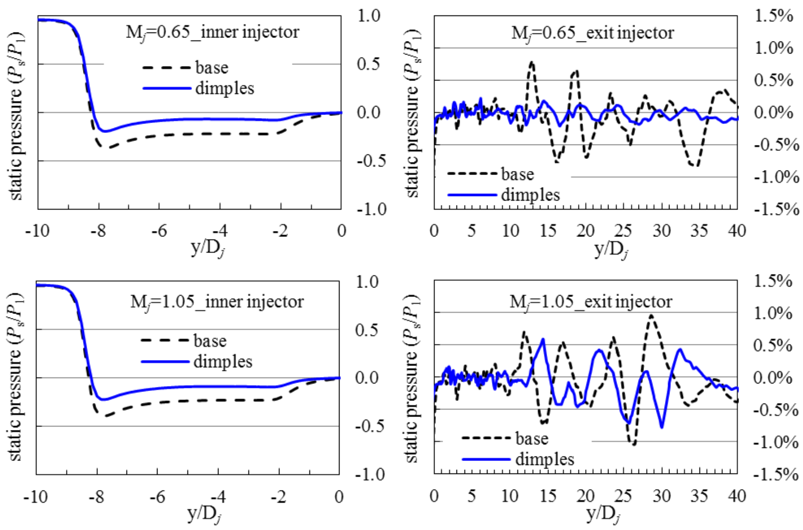

Fig.5. Oscillation of static pressure along jet centreline

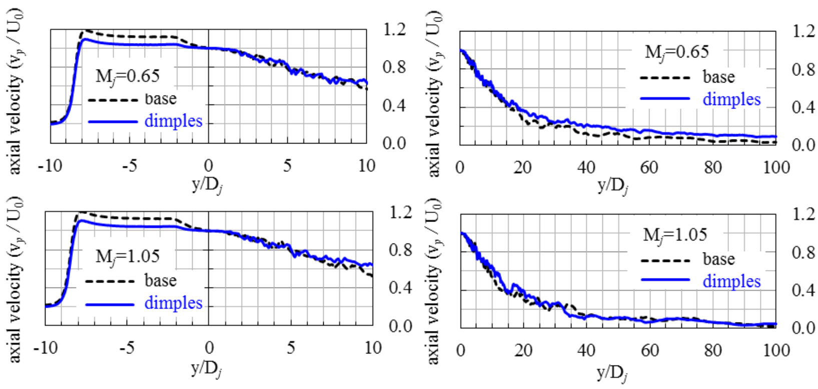

Fig.6. Reduction of axial velocity along jet centreline

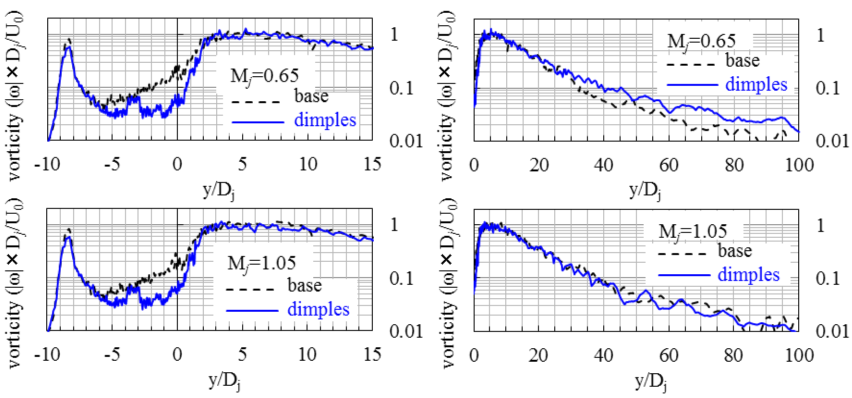

Fig.7. Variation of logarithmic vorticity magnitude along jet centerline

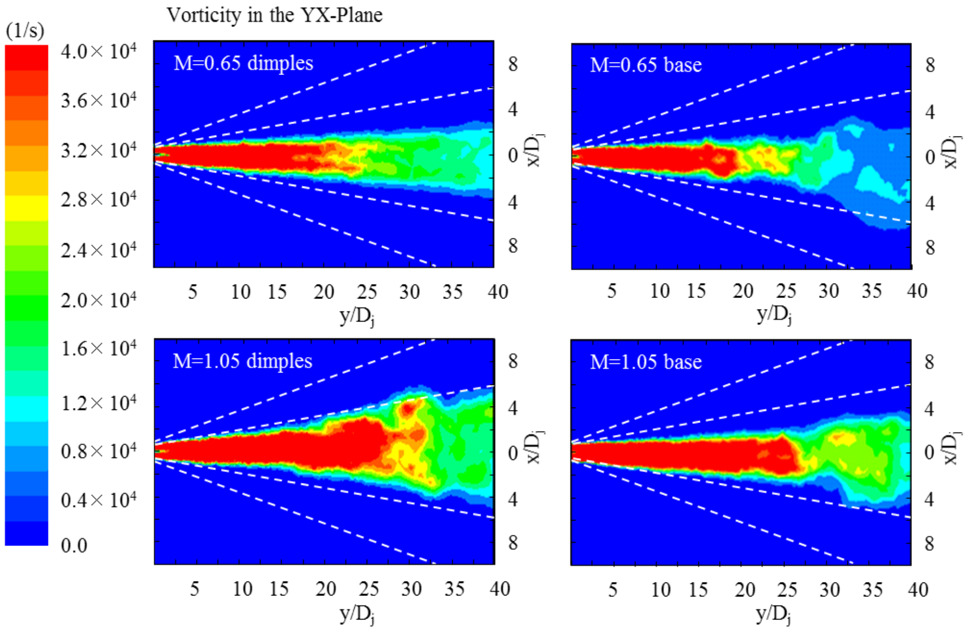

Fig.8a. Contours of vorticity near nozzle exit in the xy-Plane at z=0

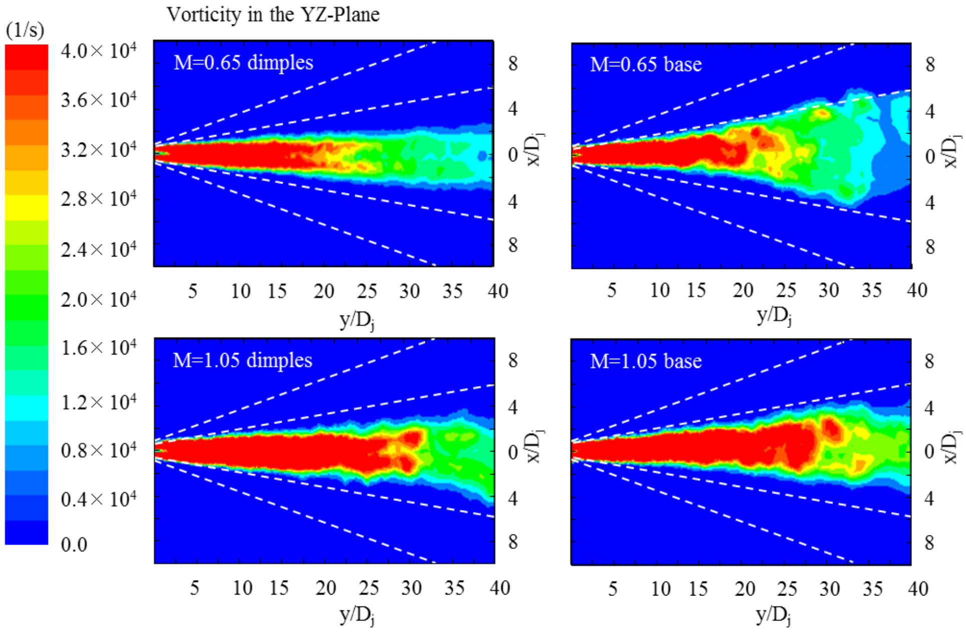

Fig.8b. Contours of vorticity near nozzle exit in the zy-plane at x=0

Moreover, as shown in the influence of dimples configuration nozzle on the structure of turbulent jet flow, four distinct zones in the region of nozzle exit have been divided with related to axial velocity decay from many studies (e.g. Yue, Z., [23])., in the paper, the variation of centerline vorticity is described in each zone of jet flow as shown in Fig.9. Immediately downstream of the nozzle is called is convergent zone (potential core) of the jet where the axial velocity is equal to the nozzle outlet, jet turbulence is confined to the annular shear layer which surrounds the potential core, and the centerline vorticity does not change also in the zone, as a simulation result, the length of the generalized potential core (the region with uniform centerline velocity ~ 99% U_0, where U_0 is axial velocity at nozzle exit of the jet-flow) is about $0.74D_j$ for base nozzle and $1.25D_j$ for dimples nozzle in case of M_j=0.65, 0.75 D_j

for base nozzle and 1.34D_j for dimples nozzle in case of M_j=1.05, respectively, it shows that the length of potential core was extended by drag reduction effect of dimples configuration. After the potential core of jet ends the axial velocity falls downstream of this point, which velocity decay can be approximated as proportional to $y^{-0.5}$, where y is the axial distance from nozzle exit), and an intermediate zone (so called transition region) appears, where the large-scale eddies which are generated with the rolling-up of the annular shear layer states to mix, and the centerline vorticity starts to increase rapidly, then fully mixed at maximum valve of centerline vorticity, from the simulation results, fully mixed (which is defined as logarithmic of $|\omega|\times D_j / U_0 \sim 0.9$) at y/D_j = 3.98 for base nozzle and y/D_j = 5.24 for dimples nozzle in case of subsonic jet (M_j=0.65), y/D_j = 7.66 for base nozzle and y/D_j = 3.40 for dimples nozzle in case of supersonic jet (M_j=1.05), respectively, it indicates that the dimples configuration enhances mixing rate of turbulent eddies at centerline in case of supersonic jet (M_j=1.05), and delays mixing speed of turbulent eddies in case of subsonic jet (M_j=0.65). however, the intermediate region of jet is often regarded as the region of the dominant noise generation.

Beyond the fully mixed point, the turbulent flow towards the self-similar zone jet, the centerline vorticity starts to reduce, the axial velocity decay is approximated as proportional to $y^{-1.0}$. And the last zone of turbulent jet flow is termination zone, the rates of evolution of the flow field and turbulent fluctuations are quite different, the actual mechanisms in this zone are not understood properly.

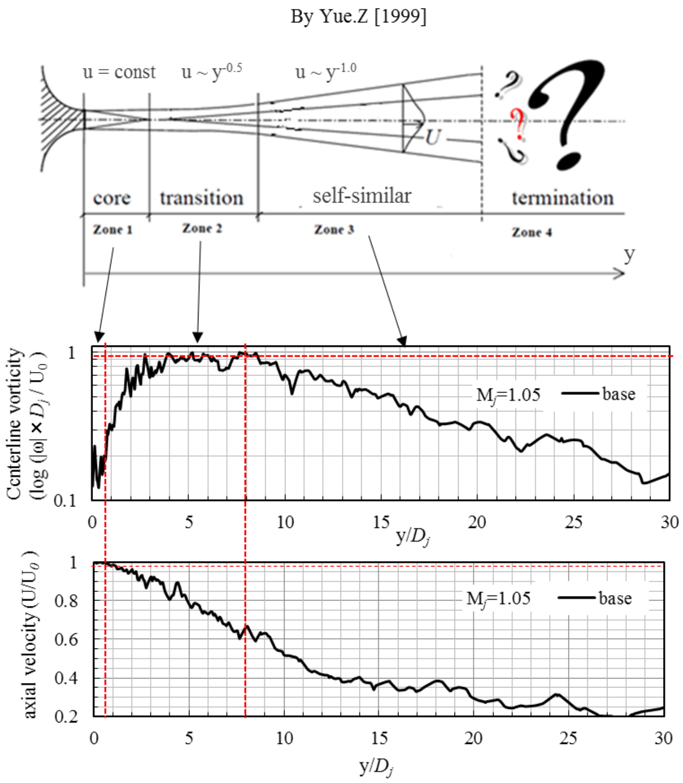

Fig.9 Four distinct zones region of nozzle exit

3.2. *Results of Acoustic Field*

In FLUENT version 14.5, results of acoustic field are obtained by the permeable FW-H surface integral method, using acoustic signals files with stocked time histories of jet flow field variables on the selected surface, the acoustic signals file was stocked at every 10 time steps of LES unsteady air jet flow simulation, and total 2000 files are used for acoustic computation.

3.2.1. Effect of FW-H surface on acoustic results

Figures 10 give the comparisons of spectrum of sound pressure level (SPL) at several observation points (observer angle = 30, 60, 90, 120, 150) in the different FW-H, it shows that the acoustic results is difference in particular lower frequency of both base nozzle and dimples nozzle at all observer angle, it is clear that the acoustic computation should select larger integral surfaces with conical divergence of S_2=50 deg., which encloses all quadrupoles source from large scale turbulence of turbulence jet flow as shown in Fig.8 again.

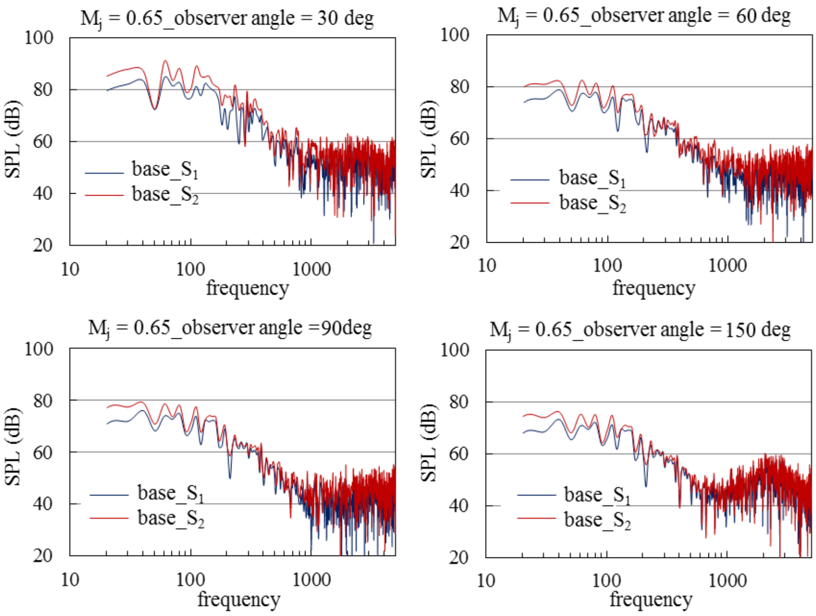

Fig.10a Effect of FW-H surface on acoustic results in case of M_j=0.65

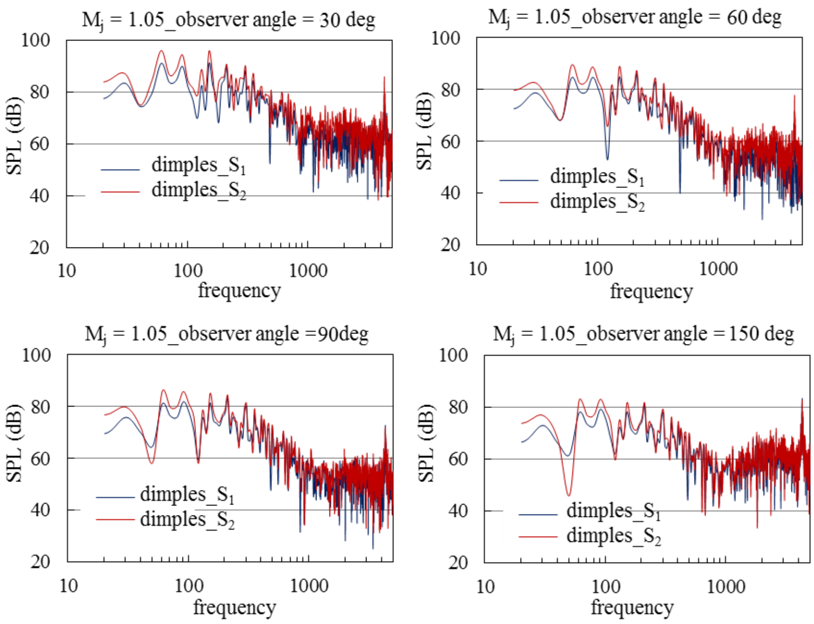

Fig.10b Effect of FW-H surface on acoustic results in case of M_j=1.05

3.2.2. Acoustic results with variation of observer angles

Jet noise reduction effect of dimples nozzle in the all observer points (from 10 to 170 deg.) are plotted as shown in Fig.11, it can be found that noise reduction effect of dimples nozzle is only valid in case of subsonic jet (M_j=0.65), especially in the zone of high frequency noise. Conversely, the jet noise is increased behind of nozzle exit (at observer angles 120 and 130 deg.) in case of dimples nozzle for supersonic jet (M_j=1.05), due to the notch lip of dimples nozzles exit, in which the notch itself caused additional noise by increasing the sound pressure level at the nozzle exit.

In addition, Fig.12 compares the spectrum of sound pressure level with base nozzle and dimples nozzle at observer angles 30, 60, 90, 120, 150deg., it also shows the differences in noise spectrum with variation zone of observer angles, it means that distinct physical mechanisms of jet noise should exist, noise from subsonic jets is mainly due to turbulent mixing, and two jet noise source are fine-scale turbulence structures at larger observer angle and larger-scale turbulent structures at small observer angle, which the high frequency noise increases at lager observer angle and is un-variant at small observer angle. Supersonic jet noise consists of three main components, the first source is Mach wave emission (turbulent mixing noise) which dominates in the downstream of jet flow, the second source is screech tones for observer angles behind jet exit, the third source is broadband shock noise at observer angles near jet exit, the latter two noise components are generated only when the jet is imperfectly expanded and a shock cell structure is formed in the jet plume (see image graphic Fig.13 by B. Henderson [24]), moreover, in case of C-D (Convergent-Divergent) nozzle, transonic tones which is generated by internal shock cell structure of nozzle effects all observer angles, and the frequency of that is differs from the frequency of screech tones (Zaman[25]), however, in the present study, the high pick value which is considered as transonic tones is clearly visible at the high frequency (~ 4318 Hz) in case of dimples nozzle for supersonic jet (M_j=1.05), due to the internal shock cell structure in tube inlet of injector as shown in Fig.14, and despite the fact that the internal shock cell structure is also occurred in case of base nozzle, the transonic tones is not found within ranges of less than 5000 Hz, the reason for this can be considered that the dimples shape on the nozzle surface reduces the inflection from internal wall of nozzle, which is advantageous for transonic tones propagation in the nozzle.

Furthermore, Fig.15 compares the results of base nozzle with predictions from the Michel model [26] and the experimental data by Tam [10] for a Mach number M ($\equiv U_0/a_0$) = 0.9 jet, for the variation tendency of SPL with observer angles changes, the aeroacoustics characteristics with observation angle are in qualitative agreement with those published data.

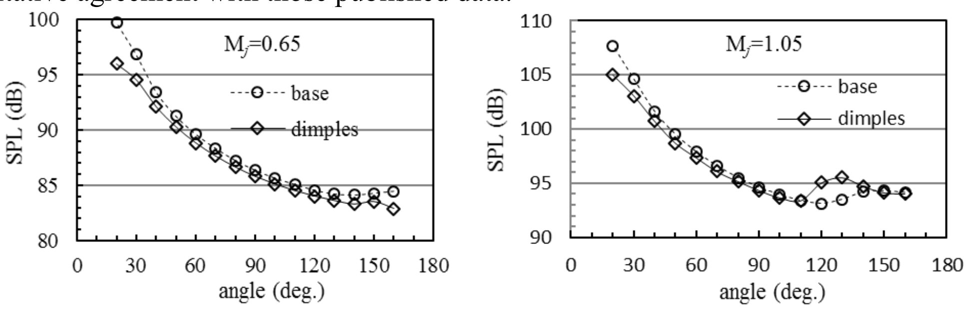

Fig.11 Jet noise reduction effect of dimples nozzle in the all observer points

IOP Conf. Series: Materials Science and Engineering **249** (2017) 012009 doi:10.1088/1757-899X/249/1/012009

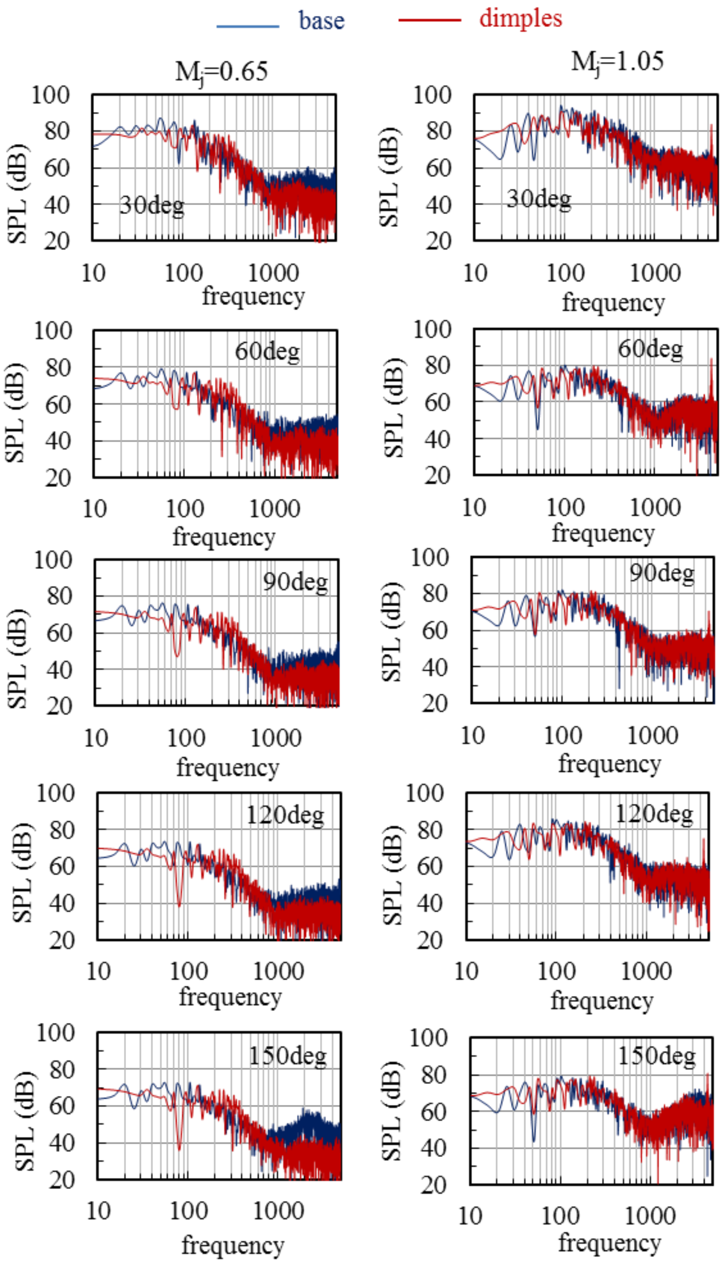

Fig.12 Compares spectrum of sound pressure level with base nozzle and dimples nozzle

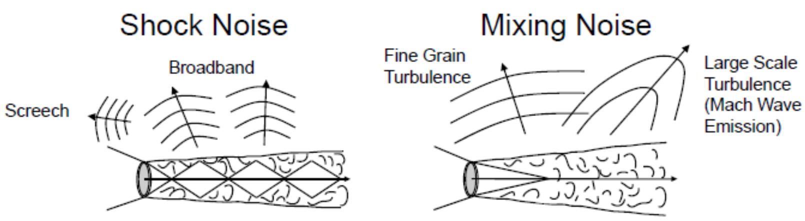

Fig.13 Jet noise sources by B. Henderson [24]

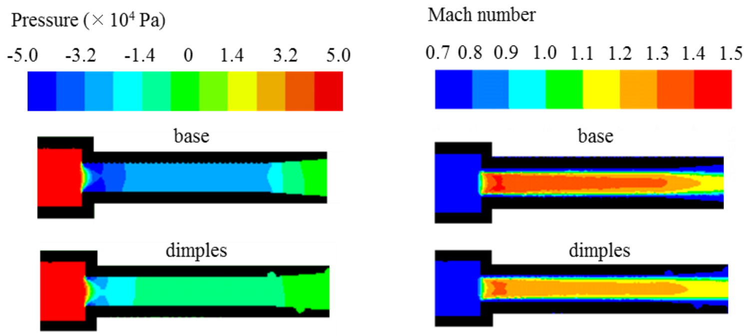

Fig.14 Internal shock cell structure in tube inlet of injector in case of M_j=1.05

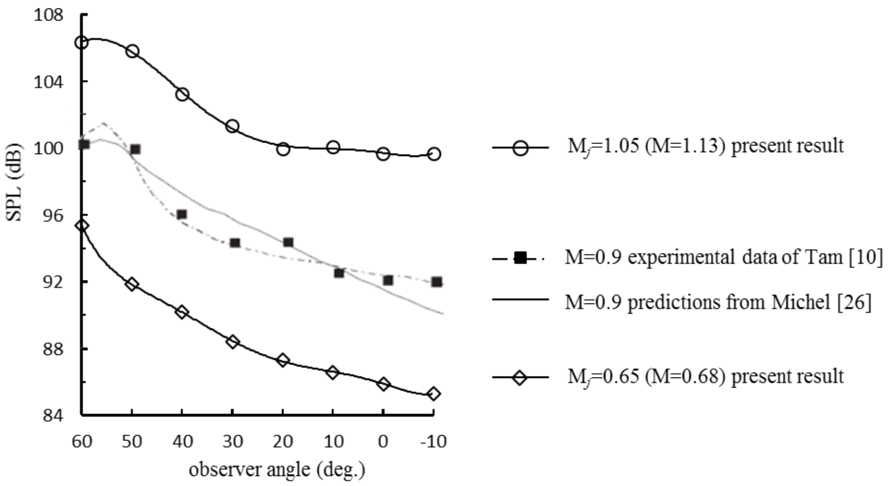

Fig.15 Comparison with Michel model and experimental data for a Mach number M =0.9 jet.

4. Conclusion

In the paper, jet noise computation of an air micro-injector with dimples shape on the inner surface of divergent nozzle is carried out in case of subsonic and supersonic jet flow, using LES/FW-H simulation method, and the influence of dimples nozzle effect on the turbulent jet flow and the jet noise reduction effect of dimples shape are numerically investigated. As for results, the noise reduction effect of dimples nozzle is only confirmed in case of subsonic jet, in which the fine-scale turbulent structure near jet exit becomes weak due to drag force reduction effect of dimples nozzle, and conversely, the jet noise level of dimples nozzle is increased in case of supersonic jet, because the dimples shape disorders the jet flow and enhances turbulent structures near jet exit.

5. References

[1] Lighthill, M.J., “On sound generated aerodynamically: I. General theory,” *Proc. Royal Soc. of London A*, Vol.222, 1952, pp.564-587.
[2] Viswanathan, K., “Mechanisms of jet-noise generation: classical theories and recent developments,” *Int. J. Aeroacoustics*, Vol.8, 2009, pp.355–407.
[3] Ffowcs Williams, J.E. and Hawkins, D.L., “Sound generation by turbulence and surface in arbitrary motion,” *Proc. Royal Soc. of London A*, vol.264, 1969, pp.321-32.
[4] Mani, R., “The influence of jet flow on jet-noise, parts 1 and 2,” *J. Fluid Mech.*, Vol.73, 1976, pp.753–793,
[5] Colonius, T., Lele S. K., Moin, P., “Sound generation in a mixing layer,” *J. Fluid Mech.*, Vol.330, 1997, pp.375–409.
[6] Goldstein, M. E., “A generalized acoustic analogy,” *J. Fluid Mech.*, Vol.488, 2003, pp.315–333.

[7] Colonius, T., and Lele, S. K., "Computational Aeroacoustics: Progress on Nonlinear Problems of Sound Generation," *Prog. Aerospa. Sci.*, Vol.40, 2004, pp.345-416.
[8] Tam, C. K. W., Golebiowski, M. & Seiner, J. M., "Two components of turbulent mixing noise from supersonic jets," *In 2nd AIAA/CEAS Aeroacoustic Conf.*, State College, PA, 6–8 May 1996. AIAA-96-1716.
[9] Tam, C. K. W., Auriault, L., "Jet mixing noise from fine scale turbulence," *AIAA Journal*, Vol.22, 1999, pp.145–153.
[10] Tam, C. K. W., Viswanathan, K., Ahuja, K. K., and Panda, J., "The Sources of Jet Noise: Experimental Evidence," *J. Fluid Mech.*, Vol. 615, 2008, pp. 253–292.
[11] Morris P. J., Farassat F., "Acoustic analogy and alternative theories for jet-noise prediction," *AIAA Journal*, Vol.40, 2002, pp.71–680
[12] Morris P. J., "A note on noise generation by large scale turbulent structures in subsonic and supersonic jets," *Int. J. Aeroacoustics*, Vol.8, 2009, pp.301–316.
[13] Viswanathan, K., "Aeroacoustics of hot jets," *J. Fluid Mech*., Vol.516, 2004, pp.39-82.
[14] Freund, J. B., Lele, S.K. and Moin, P., "Numerical Simulation of a Mach 1.92 Turbulent Jet and Its Sound Field", *AIAA Journal*, Vol.38, No.11, 2000, pp.2023-2031
[15] Freund J. B., "Noise sources in a low Reynolds number turbulent jet at mach 0.9," *J. Fluid Mech*., Vol.438, 2001, pp.277–305
[16] Ali Uzun and M. Yousuff Hussaini, "Simulation of Noise Generation in the Near-Nozzle Region of a Chevron Nozzle Jet," *AIAA Journal*, Vol.47, No.8, 2009, pp. 1793-1810.
[17] Viswanathan, K., Shur M.L., Spalart P.S., Strelets M.Kh., "Numerical prediction of noise from round and beveled nozzles," CD-ROM, *Proc.of Euromech Colloquium*, Vol.467: "Turbulent Flow and Noise Generation", Marseille, France, July 18-20, 2005.
[18] Michael L. Shur , Philippe Spalart , Michael Strelets, "Noise Prediction for Increasingly Complex Jets. Part I, Methods and tests; Part II, Applications," *Int.J. Aeroacoustics*, Vol.4, No.4, 2005, pp.247-266.
[19] Bodony, D. J. and Lele, S. K., "Jet Noise Prediction of Cold and Hot Subnoic Jets Using Large-eddy Simulation," AIAA Paper No. 2004-3022, May 2004
[20] Nichols, J. W., Ham, F. E. & Lele, S. K., "High-fidelity large-eddy simulation for supersonic rectangular jet noise prediction," AIAA Paper 2011-2919, 2011.
[21] Junhui Liu, K. Kailasanath, Ravi Ramamurti, David Munday, Ephraim Gutmark, and Rainald Lohner, "Large-Eddy Simulations of a Supersonic Jet and Its Near-Field Acoustic Properties," *AIAA Journal*, Vol. 47, No. 8 (2009), pp. 1849-1865.
[22] Werner, H. and Wengle, H., "Large-eddy simulation of turbulent flow over and around a cube in a plate channel," *Proc. 8th Symp. On Turbulent Shear Flows*, Munich, Germany, pp.19.4.1-19.4.5, 1991.
[23] Yue, Z., "Air jet velocity decay in ventilation applications," Installationsteknik Bullettin, 1999, n. 48, ISSN 0248-141X.
[24] Henderson, B., Norum, T., "Impact of Air Injection on Jet Noise," NASA-REPORT, No.20080002268, Fall Acoustics Technical Working Group, December 4 –5, 2007, Cleveland, OH.
[25] Zaman, K.B.M.Q., Dahl, M.D., Bencic, T.J., and Loh, C.Y., "Investigation of a Transonic Resonance with ConvergentDivergent Nozzles," Journal of Fluid Mechanics, Vol. 263, 2002, pp. 313-343
[26] Michel, U., "The role of source interference in jet noise," AIAA Paper 2009-3377, *In 15th AIAA/CEAS Aeroacoustics Conf.*, 11–13 May 2009, Miami, FL.